Layer-by-layer growth in noise-reduced growth models

L. Brendel,[1,2] H. Kallabis,[1,2] and D. E. Wolf[2]
[1]*Höchstleistungsrechenzentrum, Forschungszentrum Jülich, 52425 Jülich, Germany*
[2]*FB 10, Theoretische Physik, Gerhard-Mercator-Universität Duisburg, 47048 Duisburg, Germany*
(Received 21 November 1997)

For several discrete growth models, the damping time of layer-by-layer growth, manifesting itself in oscillations of the surface width, will be related to parameters appearing in the corresponding continuum equations. The control parameter in all cases is the so called *noise-reduction parameter m*. The damping time depends on *m* with power laws determined by the continuum equations. The Eden model (versions A and B), and models related to molecular beam epitaxy are considered. [S1063-651X(98)08706-6]

PACS number(s): 81.15.−z, 05.50.+q, 68.55.−a

I. INTRODUCTION

For crystal growth on high symmetry surfaces, one can observe a technologically important growth mode, layer-by-layer growth. For a suitable choice of growth rate and temperature, quantities like the reflected high-energy electron diffraction intensity, which are sensitive to the surface morphology, show oscillations with a period of 1-ML deposition time. These oscillations are usually damped, and one of the important unsolved questions of layer-by-layer growth concerns the origin of this damping.

One possible reason commonly held responsible for the damping of the oscillations is kinetic roughening; however, other mechanisms also have to be considered, like inhomogeneous deposition or mound formation due to Ehrlich-Schwoebel barriers [1,2]. In this paper, we consider damping due to kinetic roughening.

Two physical situations will be studied: In molecular beam epitaxy (MBE), layer-by-layer growth requires that nucleation on terraces which are smaller than a certain linear dimension ℓ is essentially forbidden. Then ℓ can be identified with the diffusion length of adatoms. Atoms are deposited with a rate F, and desorption may be neglected. Therefore, on large scales these growth processes are described by continuum equations of the type [3]

$$\partial_t h = -\vec{\nabla}\cdot\vec{J} + F\ a_\perp a^d + \eta, \tag{1}$$

with the shot noise η, the surface current $\vec{J}$, which is a functional of the thickness h of the growing film, and the lattice constants $a_\perp$ and a in the growth direction and the d lateral directions, respectively. In this paper we study layer-by-layer growth in three models of this kind: The Edwards-Wilkinson (EW) model [4,5], the Wolf-Villain (WV) model [6] and the ''1+'' model of Das Sarma and Tamborenea [7].

The second class of models considered in this paper can be motivated by facet growth from a melt. Under appropriate conditions, the nucleation of a new layer happens with a small probability, because atoms are not sufficiently strongly bound to the terraces. However, once an island has nucleated, its lateral growth is essentially deterministic, because the edges are good adsorption sites for atoms from the melt. This situation has been modeled by the polynucleation growth (PNG) model [8–10]. One can obtain layer-by-layer growth oscillations in this case, too, if nucleation events are forbidden within a sufficiently large distance ℓ from existing steps [11]. ℓ could be interpreted as the diffusion length before an adsorbed atom goes back into the melt. The kinetic roughening in this physical situation is described on large scales by the Kardar-Parisi-Zhang (KPZ) equation [12], which cannot be written in the form of Eq. (1):

$$\partial_t h = \nu\vec{\nabla}^2 h + \lambda(\vec{\nabla}h)^2 + F\ a_\perp a^d + \eta. \tag{2}$$

The λ term describes a tilt dependence of the growth velocity, while the ν term represents the so called surface stiffness. Instead of PNG, in this paper we investigate layer-by-layer growth in two other models of this kind, namely, two versions of the Eden model [13].

A. Coarse graining and noise reduction

The existence of a characteristic distance ℓ, below which terraces remain flat, means that the shot noise is effectively averaged out over an area ℓ^d. The small scale diffusive dynamics responsible for this averaging is not interesting in the context of kinetic roughening. Without specifying it any further, one may try to model the growth kinetics directly on scales larger than ℓ. This coarse grained modeling of growth processes [14] is a special refinement of the more general technique called noise reduction [15,16].

In noise reduced growth models, the lattice consists of cells which can contain up to m particles and correspond in the picture of coarse graining to a volume $\ell^d a_\perp$. The fast kinetics (of whatever origin for each model), which guarantees that in a partially filled cell all particles are arranged within a single atomic layer, is not specified, and thus not implemented explicitly. The growth rules of the model only determine the transfer of a mobile particle from one cell to an adjacent one. In the simplest cases considered in this paper, these rules only depend on whether a cell is full or can still receive particles, but not on the degree to which a partially filled cell is occupied.

The technical realization is done by installing a counter in each cell to register the arrival of a particle. Only when m of them are collected is that cell is treated as occupied, which has consequences on its neighborhood depending on the model's rules. As shown below, the strength of the shot

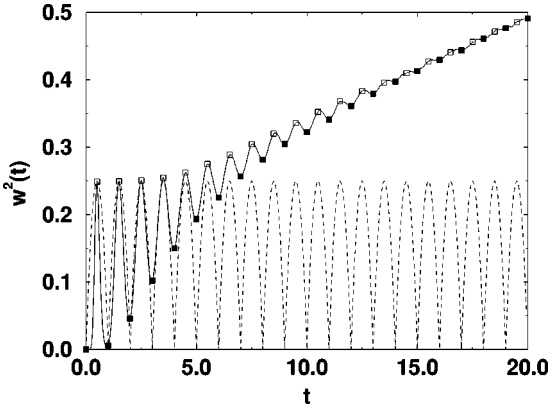

FIG. 1. Oscillations of the surface width w^2 for the Eden model (version A) with a noise reduction parameter $m=32$. Filled symbols emphasize integer times (in monolayers), open symbols half-integer times. The dashed line shows perfect layer-by-layer growth: The oscillations persist. Here and in the following figures, w is measured in units of the vertical lattice constant $a_\perp$, and t is measured in units of the layer completion time τ.

noise will decrease as m^{-1} using this technique. This explains why it is called noise reduction.

B. Oscillations of the surface width

In the ideal case of perfect layer-by-layer growth, a new layer only starts if the preceding one is completely filled, i.e., there are never more than two exposed layers. Therefore, the squared surface width $w^2=\overline{h^2}-\overline{h}^2$ (the bar denotes spatial average) oscillates as $w^2(\theta)=\theta(1-\theta)$ (cf. Fig. 1), where θ is the coverage of the top layer [17].

In reality, the layers do not grow one after another, but small islands can emerge on large islands, before their coalescence is completed. After some time there are many exposed layers and one cannot distinguish between integer and half-integer times: The oscillations are damped out, as shown in Fig. 1. The purpose of this paper is to present a theory for the dependence of the damping time $\tilde{t}$ on the noise reduction parameter m.

II. COMPUTER SIMULATION RESULTS

A. Eden models

The Eden model, introduced in 1958 [18] to describe growth of cell colonies, exists in three different variants [13]. Though in all three cases the growth of a cluster takes place by occupying a perimeter site (empty site next to an occupied one) chosen at random, the particular choice differs:

Version A. All free perimeter sites have the same probability to be chosen. The chosen site is then occupied.

Version B. All ''bonds'' connecting a free perimeter site to the cluster have the same probability to be chosen. The site belonging to the chosen bond is occupied.

Version C. All cluster sites which have neighboring free perimeter sites have equal probability to be chosen. Among the free neighbors of the chosen cluster site, the one to be occupied is again chosen with equal probability. This version will not be discussed in this paper.

In 1987, Kertész and Wolf [17] applied the noise reduction technique to versions A and C, and found that it improves the scaling behavior and causes layer-by-layer growth. For the latter they found a linear relationship between the damping time $\tilde{t}$ and the noise reduction parameter m: $\tilde{t}\propto m$.

TABLE I. The corrections to the exponent μ for the Eden models.

m	ϵ_A	ϵ_B
16	–	0.008
32	–	0.013
64	0.006 25	−0.008
128	0.005 02	–
256	−0.001 04	–

In our simulations of versions A and B, we confirmed a power law dependence $\tilde{t}\propto m^{\mu}$. The exponents were extracted by calculating $\mu(m)\equiv\log_2\tilde{t}(m)-\log_2\tilde{t}(m/2)$. The result for version A is $\mu(m)=1.1+\epsilon_A(m)$, where the small deviations ϵ are given in Table I. The corresponding data collapse is shown in Fig. 2. To point out the sensitivity of such a data collapse, a plot with $\mu=1.0$ is shown in Fig. 3. Similarly, for version B we obtained $\mu(m)=1.6+\epsilon_B(m)$ (cf. Fig. 4).

An interesting fact is that version B exhibits a different damping exponent ($\mu=1.6\pm0.02$ as shown in Fig. 4) than versions A and C, though their asymptotic scaling behavior is described by the same roughness exponent ζ and dynamic exponent z as version B, namely, those of the KPZ universality class [13,19]. This rules out the universal validity of a scaling relation between the damping exponent and the scaling exponents, as for example the relation

$$\mu=\frac{z}{2\zeta}, \tag{3}$$

first found for the noise reduced *single step model* [20].

In summary, details which do not influence the universality class may influence the scaling of the damping time with m.

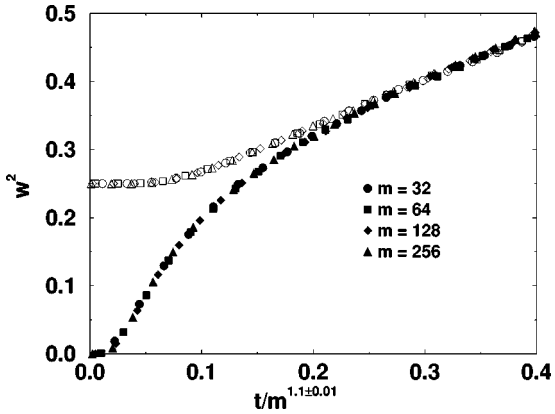

FIG. 2. Data collapse with four different noise reduction parameters showing the damping time of the Eden model (version A). Filled symbols correspond to integer times, open symbols to half-integer times. For the uncertainty ±0.01, cf. Table I.

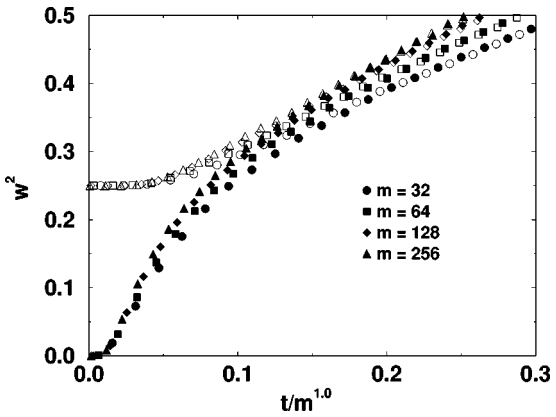

FIG. 3. A linear rescaling shows that the damping exponent for version A is not simply $\mu=1$.

B. Models related to molecular beam epitaxy

One of the basic assumptions for ideal MBE is the lack of desorption of particles back into the vacuum, as well as the absence of holes and overhangs, the ''solid on solid'' (SOS) restriction. An additional feature is the surface diffusion, which in the case of the models described below reduces to a relaxation step just after the deposition.

1. Edwards-Wilkinson model

In a lattice model suggested by Family [5], particles are deposited one by one at randomly chosen sites, and move to the lowest nearest neighbor site. Possible microscopic reasons for this downward motion in the context of molecular beam epitaxy are funneling, kick-out at terrace edges, and the influence of surfactants (see Sec. IV). A continuum version of this model had previously been investigated by Edwards and Wilkinson [4] in the different context of sedimentation in a gravitational field. The lattice version is the best known representative of the EW universality class (see Fig. 5).

Figure 6 shows the growth oscillations of the noise reduced EW model. The rescaling of time gives a damping exponent of $\mu=2.05\pm0.05$.

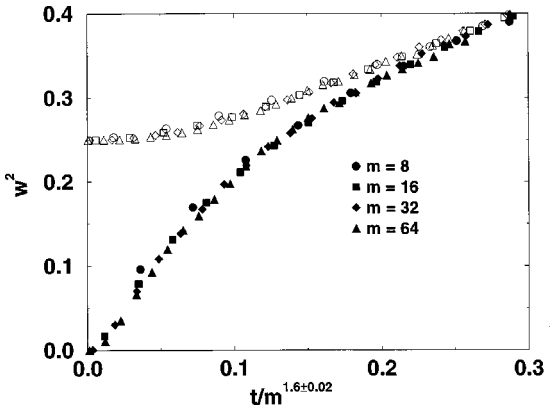

FIG. 4. Data collapse with four different noise reduction parameters showing the damping time of the Eden model (version B). Filled symbols correspond to integer times, open symbols to half-integer times. For the uncertainty ±0.02, cf. Table I.

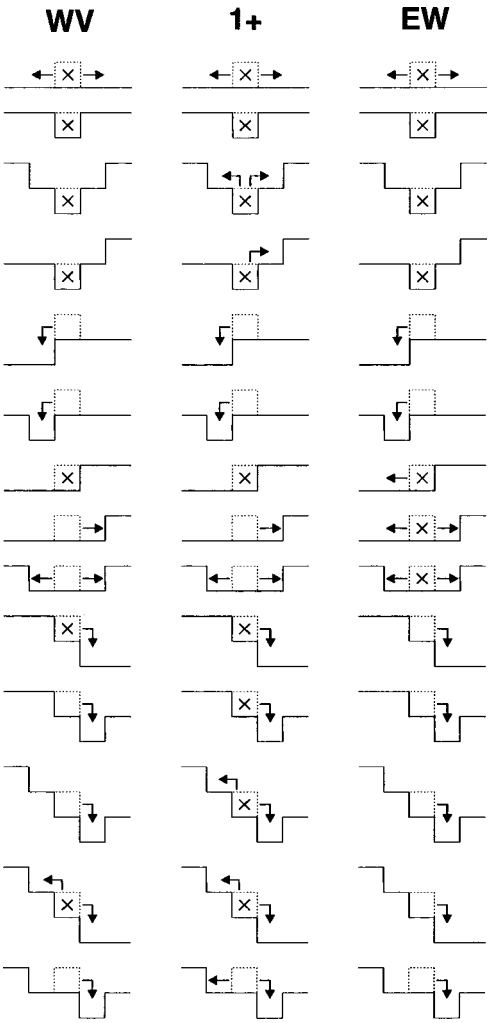

FIG. 5. The most important situations, showing the differences in the rules for the WV, 1+, and EW models, respectively. $\times$ denotes the case where the particle should stay at its location of deposition. Whenever there are two or three possible cases, one of them is chosen with probability $\frac{1}{2}$ or $\frac{1}{3}$, respectively. It should be noted that in all three models the rules were slightly modified: In a tie situation involving the deposition site, a random choice is made among the best, whereas in the original models the deposition site was taken.

2. Wolf-Villain model

In this model [6], particles do not move to the lowest nearest neighbor site but to the one with the largest number of bonds (see Fig. 5). The question of the universality class for the WV model has been debated for a long time. Recently it was shown to exhibit EW behavior after a very long crossover time ($>10^6$ ML) [21]. Figure 7 shows its damping exponent to be $\mu=1.5\pm0.05$.

3. 1+ model

This model [7] is very similar to the WV model with surface dimension $d=1$. However, sites offering three or two bonds are not distinguished; see Fig. 5.

Though the diffusion rules differ only slightly from the WV rules, the 1+ model behaves differently, especially regarding the surface current and step-height distribution (cf. Refs. [22,23]), and its connection to any universality class is

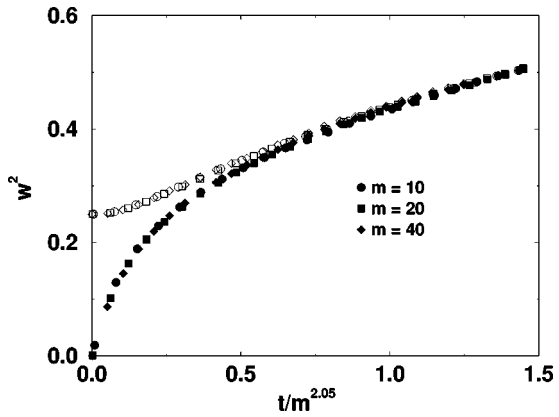

FIG. 6. Data collapse with three different noise reduction parameters showing the damping time of the EW model (random deposition with surface relaxation). Filled symbols correspond to integer times, open symbols to half-integer times.

still unclear. However the damping exponent is the same as for the WV model ($\mu = 1.5 \pm 0.05$), as shown in Fig. 8.

III. ANALYTICAL RESULTS

The simulations show that not only the envelopes of the damped oscillations but also the later time evolution scales with the same characteristic time $\tilde{t}$. Hence the power law dependence of the number of oscillations on the noise reduction parameter m can be investigated by a dimensional analysis of the m-dependent parameters of the continuum equation which governs the surface kinetics in the kinetic roughening regime, when the oscillations are no longer observable. This of course requires that a continuum description is known.

First we have to consider the strength of the noise η, which represents the fluctuations of the deposition rate around its average value F, and which is mainly shot noise, i.e.,

$$\langle \eta(x,t)\,\eta(x',t')\rangle = \mathcal{F}\delta^d(x-x')\,\delta(t-t'), \tag{4}$$

due to the statistical independence of deposition events of individual particles. The other sources of randomness in the models we simulated are related to tie situations in the microscopic kinetics, and are neglected in the continuum descriptions.

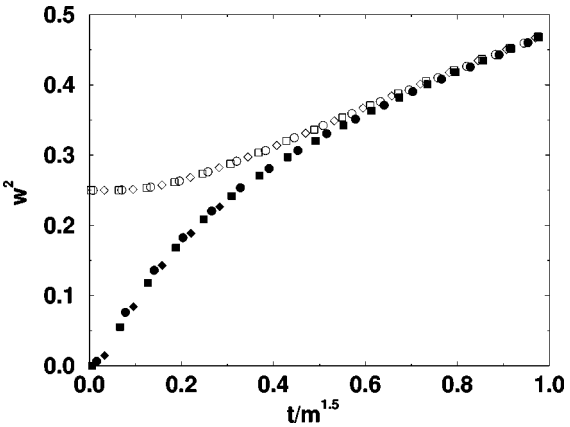

FIG. 7. Data collapse with three different noise reduction parameters showing the damping time of the WV model. Filled symbols correspond to integer times, open symbols to half-integer times.

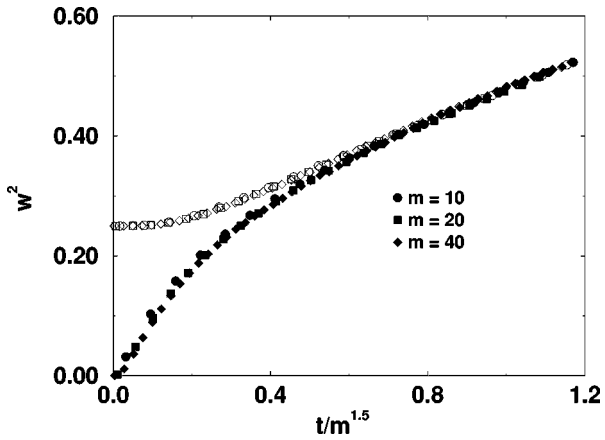

FIG. 8. Data collapse with three different noise reduction parameters showing the damping time of the 1+ model of Das Sarma and Tamborena. Filled symbols correspond to integer times, open symbols to half-integer times.

The noise strength $\mathcal{F}$ is related to the deposition rate F, even if this is removed from the Eqs. (1) and (2) by a transformation to the comoving frame ($h \to h - a_\perp t/\tau$). Here we have introduced the layer completion time τ with $1/\tau = F a^d$.

Without noise reduction, we obtain (see, e.g., Ref. [24])

$$\mathcal{F} = F\ (a_\perp a^d)^2. \tag{5}$$

When noise reduction is applied, this is no longer true, but we obtain an m dependence of $\mathcal{F}$ [17],

$$\mathcal{F} \propto 1/m. \tag{6}$$

The reason for this is that, during the deposition of t layers, each cell receives $mt \pm \sqrt{mt}$ particles which corresponds to height fluctuations of $a_\perp \sqrt{mt}/m$. According to Eq. (4), this should be $\sqrt{\mathcal{F}t/a^d}$, which proves Eq. (6).

From now on we only discuss special cases of the KPZ equation, i.e., we have to deal with the parameters $\nu(m), \lambda(m)$, and $\mathcal{F}(m)$. We neglect further terms which are responsible for crossovers, in particular for the models related to molecular beam epitaxy, where $\lambda = 0$. Some of these have been discussed elsewhere [1].

It is clear that for random deposition, i.e., in the absence of correlations between neighboring cells, layer-by-layer growth is still possible, because of the strong correlations within a cell: All m particles inside a cell are accommodated within the same layer, before the next layer can start [25]. The oscillations end when the typical height fluctuations equals about one lattice constant, i.e., $\mathcal{F}\tilde{t}/a^d \approx a_\perp$. Thus, for random deposition, one obtains [26]

$$\tilde{t} \propto m. \tag{7}$$

A. Dimensional arguments

Let us reformulate this argument in a slightly different way, which will turn out to be useful in more general situations: Let $\tilde{t}$ be the time when the typical height fluctuations $\tilde{h}$

have reached the size of the vertical lattice constant $a_\perp$. At this time $\tilde{t}$ the layer coherence will be maintained up to a characteristic length $\tilde{l}$, which in the case of random deposition is the lateral lattice constant a, but can be bigger if communication between cells is allowed. As the dimension of the noise [η] is (height)/(time), and that of the δ functions (length)$^{-d}$ and (time)$^{-1}$, respectively, it follows from Eq. (4) that

$$\mathcal{F} \sim \frac{\tilde{l}^d}{\tilde{t}} a_\perp^2, \tag{8}$$

where the sign $\sim$ means ''equal up to a dimensionless constant independent of m.'' Using Eq. (6), and solving for $\tilde{t}$, one obtains Eq. (7).

Now let us look at the EW model. Here correlations can spread among neighboring cells. The only new parameter entering the continuum description is ν. A similar dimensional argument as just given for $\mathcal{F}$ shows that

$$\nu \sim \frac{\tilde{l}^2}{\tilde{t}}. \tag{9}$$

Solving Eqs. (8) and (9) for $\tilde{t}$ and $\tilde{l}$ for $d=1$ gives

$$\tilde{t} \sim \frac{\nu}{\mathcal{F}^2} a_\perp^4, \quad \tilde{l} \sim \frac{\nu}{\mathcal{F}} a_\perp^2. \tag{10}$$

In Sec. III C we shall show that in the EW model ν is m independent for not too small m. Together with Eqs. (6) and (10), this implies

$$\tilde{t} \propto m^2, \quad \tilde{l} \propto m, \tag{11}$$

in very good agreement with our simulation results for $\tilde{t}$.

Now let us turn to the Eden model: For the ''full'' KPZ equation (i.e., $\lambda \neq 0$) we have to take the renormalization of the coefficients ν and $\mathcal{F}$ into account; λ is not renormalized [12]. Fortunately, in $d=1$ [27], the combination $\mathcal{F}/\nu$ is also not renormalized, which enables us to do the dimensional analysis in the same way as above. This leads to

$$\frac{\mathcal{F}}{\nu} \sim \frac{a_\perp^2}{\tilde{l}}, \quad \lambda \sim \frac{\tilde{l}^2}{a_\perp \tilde{t}} \tag{12}$$

or

$$\tilde{t} \sim \frac{\nu^2}{\mathcal{F}^2 \lambda} a_\perp^3, \quad \tilde{l} \sim \frac{\nu}{\mathcal{F}} a_\perp^2. \tag{13}$$

While Eq. (6) still holds true, we do not know the m dependence of ν and λ in the Eden model. Assuming the power laws

$$\nu \propto m^{e_\nu}, \quad \lambda \propto m^{e_\lambda}, \tag{14}$$

we arrive at

$$\tilde{t} \propto m^{2e_\nu - e_\lambda + 2}, \quad \tilde{l} \propto m^{e_\nu + 1}. \tag{15}$$

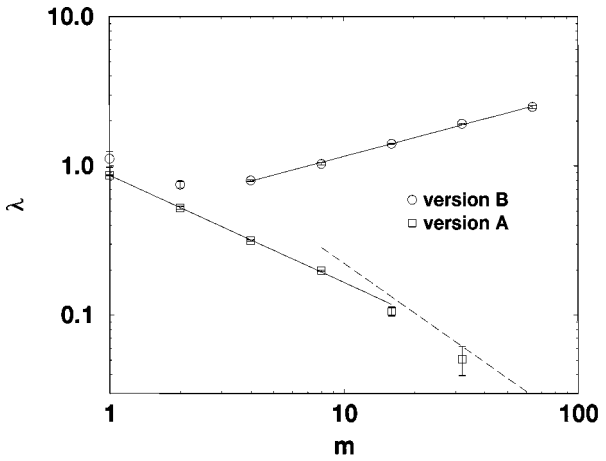

FIG. 9. The measured λ in the case of the Eden model as a function of m in a log-log plot. The slopes of the regression lines (solid) are -0.72 ± 0.01 (version A) and 0.42 ± 0.01 (version B). The dashed line corresponds to an exponent of -1.1 (cf. Sec. III B).

Now the parameter λ can be measured explicitly, since the KPZ equation is invariant under the tilt transformation

$$h(x,t) \to h(x - 2\lambda s t, t) - sx + \lambda s^2 t, \tag{16}$$

which shows, that a surface with an imposed tilt (slope s) has an additional velocity λs^2 compared to the flat one, and thus λ can be extracted from this extra velocity.

Then a variation of m allows for the determination of the exponent e_λ. Figure 9 shows that λ varies as a function of m according to a power law. Using $e_\nu = \mu/2 + e_\lambda/2 - 1$ [cf. Eq. (15)], and the numerical results for μ, e_ν can also be predicted. The results are shown in Table II. In Sec. III B, we will have another estimate for e_ν.

For version A, the signs of the exponents e_λ and e_ν can be understood in the following way: Consider a regular surface with a global tilt s, i.e., due to the discreteness a step train of terrace size $\ell = a_\perp / |s|$. If all steps are at least two lattice constants apart (i.e., $\ell \geq 2a$), there are three types of growth sites: The lower site next to a step is called a kink site, and the upper one the edge site; all the others are terrace sites. Now we apply the growth according to the Eden rules in the noise free limit (i.e., $m \to \infty$). In the absence of noise, no steps higher than two lattice constants, no overhangs, and no holes can emerge. Thus in version A each site has the same local growth velocity. Therefore, $\partial_t h(x,t)$ does not depend on the slope s. In fact it is totally independent of the surface configuration, and Eq. (2) reduces to the trivial equation

$$\partial_t h = \frac{a_\perp}{\tau}, \tag{17}$$

TABLE II. The exponents e_λ and e_ν for the Eden models.

Version	e_λ	e_ν
A	-0.72 ± 0.01	-0.81 ± 0.01
B	0.42 ± 0.01	0.01 ± 0.015

i.e., $\nu=\lambda=\mathcal{F}=0$, in accordance with negative exponents e_ν and e_λ.

In version B, according to the rules, the kink sites have twice the local growth velocity as edge and terrace sites, and hence they provide an excess velocity which is proportional to their density $|s|/a_\perp$, so that Eq. (2) becomes

$$\partial_t h=\frac{a_\perp}{\tau}+\frac{a}{\tau}|\vec{\nabla}h|. \tag{18}$$

For large but finite m, the cusp in $a/\tau|\vec{\nabla}h|$ will be rounded, and can be approximated by a parabolic part $\lambda(\vec{\nabla}h)^2+a^2/(4\tau^2\lambda)$ for $|\vec{\nabla}h|\leqslant a/(2\tau\lambda)$. Thus the cusp for $m\to\infty$ can be seen as the limit $\lambda\to\infty$, and so we have $\nu=\lambda^{-1}=\mathcal{F}=0$, in agreement with a positive e_λ, while for $e_\nu\simeq 0$ the situation is unclear.

B. Scaling

It is instructive to point out again the role of the quantities $\tilde{t}$ and $\tilde{l}$ introduced in Sec. III A. There we used dimensional arguments to find out the only way in which the parameters $\mathcal{F}$, ν, and λ can enter the proposed time and length.

Now let us take the exact solution of the EW equation in one dimension [27],

$$w^2(t,L)=\frac{\mathcal{F}}{\nu}Lf\left(\frac{\nu t}{L^2}\right), \tag{19}$$

where L is the linear dimension of the system, and the scaling function $f(x)$ behaves like $\sqrt{x}$ for $x\ll 1$, and approaches a constant for larger values.

Using relations (8) and (9) with their numerical prefactors set to 1, and reinserting the EW scaling exponents $z=2$ and $\zeta=1/2$ into Eq. (19), this can be written as

$$\frac{w^2(t,L)}{a_\perp^2}=(L/\tilde{l})^{2\zeta}\cdot f\left(\frac{t/\tilde{t}}{(L/\tilde{l})^z}\right). \tag{20}$$

This is not a new result, of course, but a more detailed version of the well known and widely used general scaling expression, first given in Ref. [28]: detailed, because it takes into account the dimensions of height, length, and time via $a_\perp$, $\tilde{l}$, and $\tilde{t}$, respectively. Apart from dimensional consistency this reminds one of the fact that the validity of power laws describing the scaling behavior is always limited from below by a cutoff value, which then serves as the natural unit. This does not play a role as long as it is fixed (e.g., the lattice constant), but in this situation the units turn out to be just $\tilde{l}$ and $\tilde{t}$, and thus depend on the parameters ($\mathcal{F}$, ν), and therefore on m.

Moreover, it was not by chance that $\tilde{l}$ appeared in Eq. (20) instead of, e.g., the lattice constant a. If a power law would already apply on scales comparable to a, there should be a change in behavior when eventually the scale of $\tilde{l}$ is reached (which is larger than a). This statement is a general one; the natural unit appearing in a power law (i.e., its lower cutoff) is the largest of all characteristic scales with the correct dimension.

Hence, with the general scaling function $f(x)$ (which varies like $x^{2\zeta/z}$ for small x), Eq. (20) is not restricted to the EW equation, and it can be used to predict the saturation behavior of w^2:

The saturation time is reached when the argument of the scaling function is of order 1, i.e.,

$$t_{\mathrm{sat}}\sim L^z\tilde{l}^{-z}\tilde{t}, \tag{21}$$

and inserting the power laws

$$\tilde{t}\propto m^\mu,\quad \tilde{l}\propto m^\kappa \tag{22}$$

yields

$$t_{\mathrm{sat}}\propto m^{\mu-z\kappa}L^z. \tag{23}$$

For times longer than t_{sat}, the width saturates as

$$w_\infty^2\propto\tilde{l}^{-2\zeta}L^{2\zeta}\propto m^{-2\kappa\zeta}L^{2\zeta}. \tag{24}$$

Two special cases arise from Eqs. (23) and (24):

(1) $\kappa=0\Rightarrow$ The saturation time varies like the damping time (i.e., $t_{\mathrm{sat}}\propto m^\mu$), while the saturation width is independent of m.

(2) $\kappa=\mu/z\Rightarrow$ The saturation time does not depend on m, while the saturation width w_∞^2 varies like $m^{-2\mu\zeta/z}$, as $w^2(t)$ does for all times $t>\tilde{t}$.

In Ref. [17], it was found that for version A of the Eden model the scaled saturation width w_∞^2/L approached a constant value of about 0.052 in a $1/m$ fashion. Thus, for a large m, version A could be a candidate for case one (i.e., $\kappa=0$). With this, we obtain $e_\nu=-1$ from Eq. (15), and that in turn predicts $e_\lambda=-\mu=-1.1$, which deviates rather strongly from the values of Table II. But it should be pointed out that the value $e_\lambda=-0.72$ therein was obtained by evaluating $\lambda(m)$ for rather small values of m. In the last two points ($m=16$ and 32), there is an indication of a crossover to a lower exponent. The expected value of -1.1 is shown as a dashed line in Fig. 9. This crossover will be discussed later (Sec. IV A).

A better agreement is obtained in the case of version B. For this model, it was found in Ref. [29] (and also in our own simulations) that the saturation time is not influenced by the noise reduction, and thus we are in class 2 (i.e., $\kappa=\mu/z$). Using the exact value $z=\frac{3}{2}$ and our result $\mu=1.6$ (cf. Table I), the result of Eq. (15) is $e_\nu=0.067$, which is well in the range of that in Table II.

Another model in class 2 is the EW model. This means with $z=2$ and $\mu\simeq 2$ that $\kappa=1$ should hold true, which fits well to the result $e_\nu=0$ of Sec. IV C.

C. Surface current in the EW model

For the EW equation, the m dependence of the occurring surface current $\vec{J}$ arises from the influence of m on ν since

$$\vec{J}=-\nu\vec{\nabla}h. \tag{25}$$

This identity results when bringing Eq. (2) into the form of Eq. (1), which is only possible for $\lambda=0$.

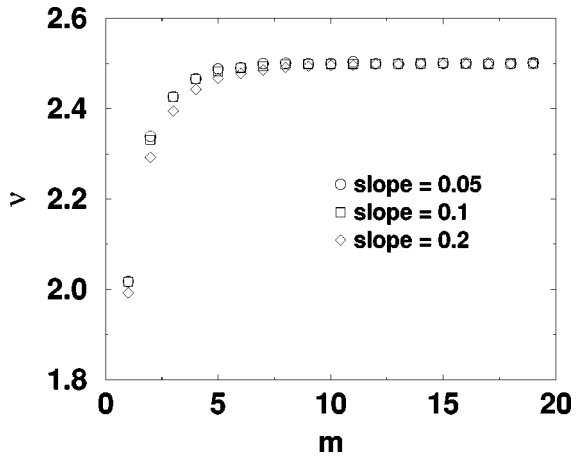

FIG. 10. The dependence of the surface current on the noise reduction parameter m for three different global tilts in the EW model. Normalizing the negative current with the tilt leads directly to the coefficient ν; cf. Eq. (25). This coefficient is independent of m for larger values of m. The limiting value $\nu=2.5$ (with units $a_\perp=a=\tau=1$) is explained in the text.

Actually the m dependence of ν is weak and vanishes for larger m, as shown in Fig. 10. The limiting value of $\nu=2.5$ (with units $a=a_\perp=\tau=1$) for $m\to\infty$ (i.e., no noise) can be explained as follows.

If we consider again a regular surface with a positive global tilt s, the contribution to the average current is -2 (along the arc length) for the edge sites, $-\frac{1}{2}$ for the kink sites (cf. Fig. 11 and Fig. 5, lines 5 and 7, respectively), and zero for the terrace sites. Since we have s steps per unit length this results in a current of $j_\infty=-5/2s$, which, when compared to Eq. (25), reveals the limiting value for ν. For lower noise reduction we obtain deviations from the perfect steps during growth. Their effect is a reduction of the current [cf. Fig. 11(c)].

IV. DISCUSSION

A. Description by continuum equations

For versions A and B of the Eden model, and for the EW model, we were able to relate the m dependence of the damping time to the m dependence of the coefficients of the corresponding continuum equations. This was done by identifying the damping time $\tilde{t}$ and the associated layer coherence length $\tilde{l}$ with the characteristic time and length scales appearing in the scaling law which follows from the continuum equations. This identification was indirectly confirmed by measuring the corresponding m dependencies explicitly.

Whereas the damping time exponent could be explained in this way for the EW model and version B of the Eden model, version A of the Eden model turned out to be more subtle, because the coefficient λ of the corresponding KPZ equation has no simple power law dependence on m (cf. Fig. 9). In this context an important property of the Eden models should be brought back into mind: the intrinsic width [19,17]. This additional contribution to the surface width has a different behavior than the long wavelength fluctuations described by Eq. (2), and thus leads to strong corrections to scaling laws like Eq. (20). Since the intrinsic width influences the growth velocity v via the perimeter density [30], direct measurements of $v(\nabla h)$ exhibit just an effective λ. Only a sufficient suppression of the intrinsic width by means of the noise reduction [17], the ''real'' behavior [i.e., according to Eq. (2)] is revealed. The same effect (yet weaker) can be seen for version B in Fig. 9: The first three data points indicate a crossover from a negative exponent to the correct one. Apparently the effect of the intrinsic width on the measured λ is more pronounced in the case of version A, for which a stronger correction to scaling is already known [13,17]. Unfortunately the desired range of larger m is difficult to access, since there the tilt dependence of the velocity becomes smaller than the error bars.

B. Microscopic considerations

Because of the lack of a suitable continuum description for the WV and 1+ models (cf. also Refs. [31,21]), their value $\mu=1.5$ will not be analyzed further here. Still, a comparison of these models with the EW model gives insight into microscopic mechanisms which have a bearing on real molecular beam epitaxy.

This is because it seems—regarding the microscopic rules—at first sight unclear why the EW and WV models should behave differently for early times. Since for an atom located at an edge site, the kink site has a lower height and at the same time a higher coordination, the atom will hop down in both cases (cf. Fig. 5, lines 5 and 6; this argument only holds true for $d=1$).

The small but crucial difference arises when the atom is deposited directly at the kink site or at the terrace site next to it: After relaxation it will be found at the kink site with a probability of $p=1$ for WV rules but only with $p=\frac{5}{12}$ for EW rules (cf. Fig. 5, lines 7 and 8). This results in a larger

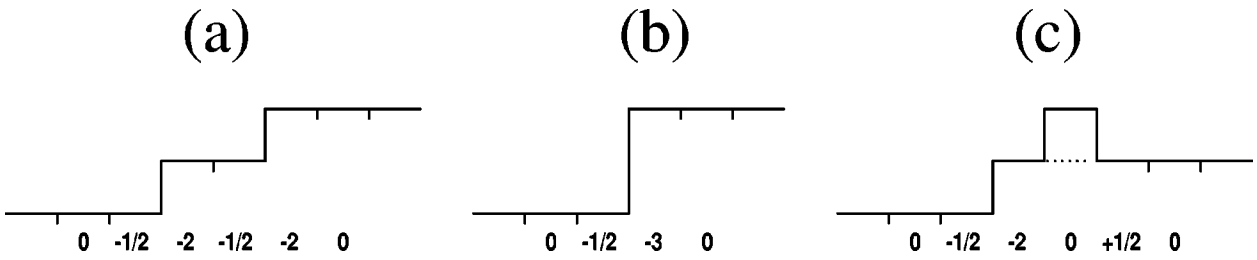

FIG. 11. Surface currents (along the arc length) for the EW model. The numbers denote the contribution of each site to the average current (with units $a=a_\perp=\tau=1$). In (a), two separated steps produce a net contribution of -5, while, in (b), for a double step, it is reduced to -3.5. (c) shows that the addition of a single atom may reduce the contribution of a step from -2.5 to -2.

island density for the EW model (i.e., in smaller islands at a fixed coverage), which increases the chance for a deposited atom to relax into the incomplete layer.

That small islands are good for layer-by-layer growth (here manifested by $\mu=2$ for EW being larger than $\mu=1.5$ for WV) is not only specific to the toy models considered here, where atoms can only escape islands when they are deposited on an edge site and the effect only becomes visible by using the noise reduction technique. Indeed, in experiments, layer-by-layer growth can be promoted by artificially increasing the density of islands (e.g., by sputtering; cf. Ref. [32]).

Moreover the difference between EW rules and WV rules can be regarded as an example for the Markov mechanism [33], by which surfactants can improve layer-by-layer growth: If the surfactant atoms preferentially attach to the kink sites, they may suppress the accretion of adatoms at a step from the *lower* terrace, but still may give way for adatoms coming down from the *upper* terrace. Thus the surfactant would make a WV-type growth more EW like. As explained above this would increase the island density and hence improve layer-by-layer growth.

ACKNOWLEDGMENTS

Useful conversations with János Kertész and Joachim Krug are gratefully acknowledged. This work was supported by the Deutsche Forschungsgemeinschaft through the Graduate College ''Structure and Dynamics of Heterogeneous Systems.''

[1] H. Kallabis, L. Brendel, J. Krug, and D. E. Wolf, Int. J. Mod. Phys. B **11**, 3621 (1997).
[2] D. E. Wolf, in *Dynamics of Fluctuating Interfaces and Related Phenomena*, edited by D. Kim, H. Park, and B. Kahng (World Scientific, Singapore, 1997), pp. 173–205.
[3] J. Villain, J. Phys. I **1**, 19 (1991).
[4] S. F. Edwards and D. R. Wilkinson, Proc. R. Soc. London, Ser. A **381**, 17 (1982).
[5] F. Family, J. Phys. A **19**, L441 (1986).
[6] D. E. Wolf and J. Villain, Europhys. Lett. **13**, 389 (1990).
[7] S. D. Sarma and P. Tamborena, Phys. Rev. Lett. **66**, 325 (1991).
[8] F. C. Frank, J. Cryst. Growth **22**, 233 (1974).
[9] G. H. Gilmer, J. Cryst. Growth **49**, 465 (1980).
[10] W. van Saarlos and G. H. Gilmer, Phys. Rev. B **33**, 4927 (1986).
[11] L. Brendel and D. E. Wolf (unpublished).
[12] M. Kardar, G. Parisi, and Y.-C. Zhang, Phys. Rev. Lett. **56**, 889 (1986).
[13] R. Julien and R. Botet, Phys. Rev. Lett. **54**, 2055 (1985).
[14] D. E. Wolf, in *Scale Invariance, Interfaces, and Non-Equilibrium Dynamics*, edited by M. Droz, A. McKane, J. Vannimenus, and D. E. Wolf (Plenum, New York, 1995), pp. 215–248.
[15] J. Szép, J. Cserti, and J. Kertész, J. Phys. A **18**, L413 (1985).
[16] C. Tang, Phys. Rev. A **31**, 1977 (1985).
[17] J. Kertész and D. E. Wolf, J. Phys. A **21**, 747 (1988).
[18] M. Eden, in *Symposium on Information Theory in Biology*, edited by H. P. Yockey (Pergamon, New York, 1958).
[19] J. G. Zabolitzky and D. Stauffer, Phys. Rev. A **34**, 1523 (1986).
[20] L.-H. Tang, in *Growth Patterns in Physical Sciences & Biology*, edited by J.-M. Garcia-Ruiz (Plenum, New York, 1993), p. 99.
[21] M. Kotrla and P. Šmilauer, Phys. Rev. B **53**, 13 777 (1996).
[22] J. Krug, Habilitation, Heinrich-Heine-Universität Düsseldorf, 1996.
[23] J. Krug, Phys. Rev. Lett. **72**, 2907 (1994).
[24] T. Nattermann and L.-H. Tang, in *Surface Disordering: Growth, Roughening, and Phase Transitions*, edited by R. Jullien, J. Kertész, P. Meakin, and D. E. Wolf (Nova, New York, 1992), pp. 13–19.
[25] L. Brendel, Master's thesis, Gerhard-Mercator-Universität-GH Duisburg, Germany, 1994.
[26] D. E. Wolf and J. Kertész, Phys. Rev. Lett. **63**, 1191 (1989).
[27] T. Nattermann and L.-H. Tang, Phys. Rev. A **45**, 7156 (1992).
[28] F. Family and T. Vicsek, J. Phys. A **18**, L75 (1985).
[29] P. Devillard and H. E. Stanley, Phys. Rev. A **38**, 6451 (1988).
[30] R. Hirsch and D. E. Wolf, J. Phys. A **19**, L251 (1986).
[31] P. Šmilauer and M. Kotrla, Phys. Rev. B **49**, 5769 (1994).
[32] G. Rosenfeld *et al.*, Phys. Rev. Lett. **71**, 895 (1993).
[33] I. Markov, Phys. Rev. B **50**, 11 271 (1994).